IV ECCOMAS Thematic Conference on the Mechanical Response of Composites
COMPOSITES 2013
A. Suleman, P. Camanho, et al. (Editors)

IN-PLANE SHEAR BEHAVIOUR OF NON-CRIMP FABRIC LAMINATES BY MEANS OF 3D FINITE ELEMENT ANALYSIS

L. M. Ferreira[*], E. Graciani[1], F. París[1]

[*]Escuela Técnica Superior de Ingenieros, Grupo de Elasticidad y Resistencia de Materiales, Universidad de Sevilla,
C/ Camino de los Descubrimientos, s/n 41092 Sevilla, España
luismmferreira@ipt.pt

[1]Escuela Técnica Superior de Ingenieros, Grupo de Elasticidad y Resistencia de Materiales, Universidad de Sevilla,
C/ Camino de los Descubrimientos, s/n 41092 Sevilla, España
egraciani@etsi.us.es

Keywords: Composites, Non-crimp fabric, Finite element models, In-plane shear behaviour.

Summary: *In order to characterize the in-plane shear behaviour of NCF laminates, experimental off-axis tensile tests of $[+45,-45]_{2S}$ laminates in different loading directions (parallel to the stitching yarns: warp-SP and normal to the stitching yarns: weft-ST) were carried out. Since the specimens were cut from the same panel, identical results were expected for both directions. However, the experimental tests showed that the shear modulus, the shear strength and the shear strain at failure are higher in the weft direction (ST) than in the warp direction (SP). To identify the cause(s) of such differences, a parametric study has been performed using a mesoscopic scale 3D FE model of the representative unit cell of a $[+45,-45]_s$ NCF laminate. The unit cell is composed by four laminas that have been stacked with the correspondent +45º and -45º orientations. Each lamina contains two half rectangular cross-section tows and resin pockets between them and in the top left and bottom right corners. The stitching yarns and the waviness induced by them in the tows have been added to the unit cell in order to evaluate their impact in the in-plane shear behaviour. The fibre waviness appears in the thickness direction across the length of the unit cell and since it is not normal to the tows it has been modelled according to a new approach. That is, the element's coordinate system of the finite elements placed in the crimped part of the tow are rotated to take into account for the waviness of the fibres. The study revealed that neither the stitching of the tows nor the out-of-plane waviness of the fibres is responsible for the significant differences found experimentally. On the other hand, the parametric study revealed that a misalignment between the nominal 0º and 90º tows of the NCF panels is what contributes the most for the differences found in the in-plane shear performance between SP and ST laminates.*

1 INTRODUCTION

In order to characterize the in-plane shear behaviour of NCF laminates, experimental off-axis tensile tests with $[+45,-45]_{2s}$ laminates in different loading directions: (parallel to the stitching yarns direction: *warp-SP* and normal to the stitching yarns: *weft-ST*) were carried out

within the FALCOM Project [1]. The differences between SP and ST laminates are illustrated in Figure 1.

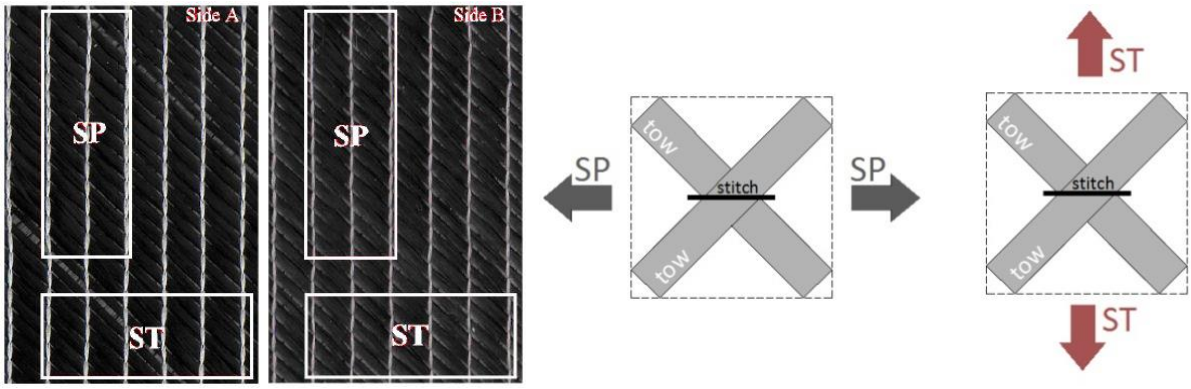

(a) (b)

Figure 1: (a) Direction of the specimen cutting [2]. (b) Schematic representation.

The NCF specimens tested were manufactured from a biaxial Tenax® HTS carbon fibre 5632 12k fabric with 534 g/m^2 by resin infusion under flexible tooling (with resin system HexFlow® RTM6).

Since the specimens were cut from the same panel identical results were expected for both directions. However, the experimental tests in the ST laminates showed higher shear modulus, shear strength and shear strain at failure (see Figure 2) than the experimental tests in the SP laminates. The results for the in-plane shear modulus G_{12} and in-plane shear strength S_{12} are presented in Table 1**Error! Reference source not found.** with V_f^l being the fibre volume fraction of the laminate.

Layup	V_f^l	**Manufacturing method**	**Direction of specimen**	G_{12} **[GPa]**	S_{12} **[MPa]**
$[+45,-45]_{2s}$	60%	RIFT	SP	$4.38^{\pm 0.43}$	$55.11^{\pm 1.91}$
			ST	$4.51^{\pm 0.34}$	$95.22^{\pm 2.95}$

Table 1: Experimental average values and standard deviations of the in-plane shear modulus G_{12} and in-plane shear strength S_{12} obtained with $[+45,-45]_{2s}$ NCF specimens in [1].

Typical experimental shear stress-strain curves obtained from the off-axis tensile test of $[+45,-45]_{2s}$ NCF laminates in both cutting directions are shown in Figure 2. Notice that the differences in the in-plane shear performance between the SP and ST laminates were also found in all the biaxial NCF laminate configurations of the specimens tested within the FALCOM project [3].

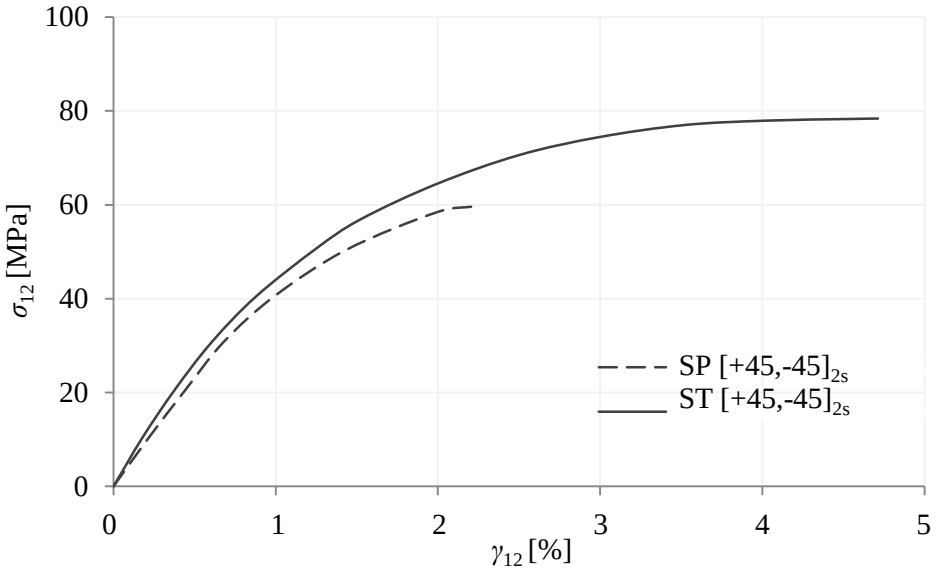

Figure 2: Typical shear stress-strain curves obtained from the off-axis tensile tests [1].

2 NUMERICAL MODELS

A mesoscopic scale 3D FE model of the representative unit cell (RUC) of a $[+45,-45]_s$ NCF laminate with the fibre crimp (due to the presence of stitching yarns) modelled with a straight mesh has been developed. Accordingly, the tows have been modelled as a homogenous material (without considering their microscopic constituents: fibre and matrix) with transversely isotropic behaviour, being the isotropic plane perpendicular to the fibres, and the resin pockets have been modelled as a homogeneous isotropic material. This RUC corresponds to the minimum unit cell that, repeated through its plane, generates a complete lamina with all its tows oriented along the same direction.

The RUC is composed by four laminas that have been stacked with the correspondent +45º and -45 º orientations, as it is shown in Figure 3(a). Each lamina contains two half rectangular cross-section tows and resin pockets between them and in the top left and bottom right corners.

In accordance with the local coordinate system represented in Figure 3, the plane of the unit cell is the 12-plane and the fibres of the +45º and -45º tows are oriented along the direction 1 and direction 2, respectively. The direction 3 corresponds to the through-thickness direction of the laminate.

The FE code used has been ANSYS® and a linear solid element SOLID45 with eight nodes and three degrees of freedom at each node (translations in the directions 1, 2 and 3) has been considered.

The geometrical parameters employed are shown in Figure 3(b), where *a* represents the length of the unit cell, *t* the thickness of each lamina and *g* the width of the gap left between two adjacent tows of each lamina. The numerical values of parameters *a, t, g* and of the fibre volume fraction of the tows V_f^t, shown in Table 2, have been obtained for $V_f^l = 60\%$. These parameters have been estimated from the internal geometry and fibre content of the materials tested [1].

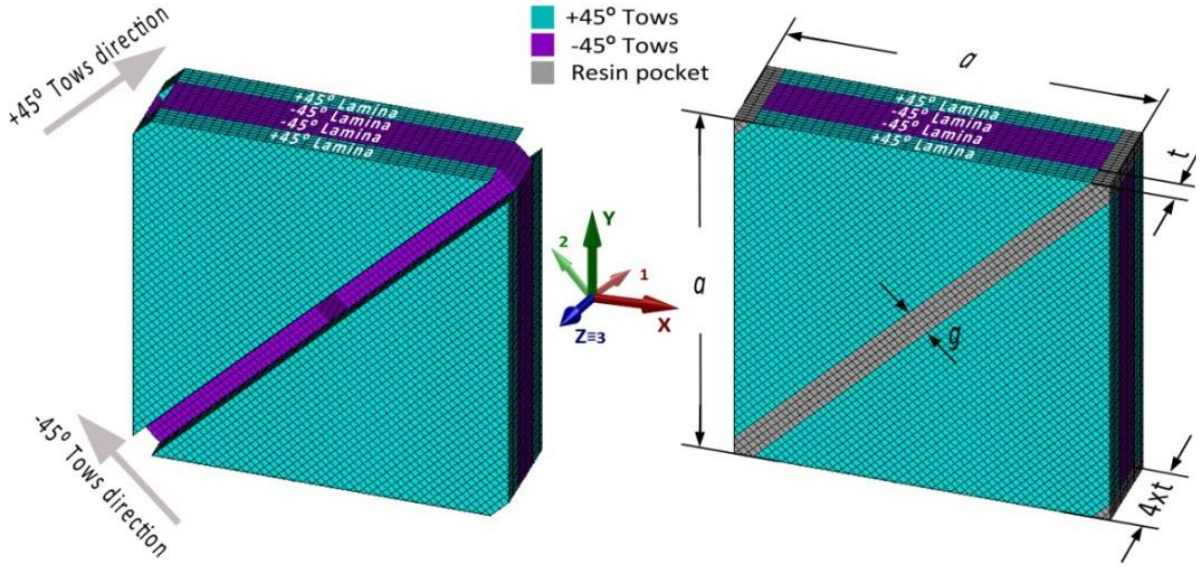

(a) (b)

Figure 3: FE model of the RUC of a $[+45,-45]_S$ NCF laminate: (a) tows shape , (b) complete FE model with dimensions employed.

V_f^l	a [mm]	t [mm]	g [mm]	V_f^t
60%	3.67	0.24	0.26	69%

Table 2: Values considered for parameters a, t, g and V_f^t in the FE model.

The SP and ST laminates are identical from the laminate theory point of view; the only difference between the laminates is the orientation of the stitching yarns regarding the load direction. In this way, the stitching yarns and the crimp induced by them have been added to the FE model in order to evaluate their impact in the in-plane shear behaviour (see Figure 4). These stitching yarns induce fibre crimp in the thickness direction [4] across the length of the RUC. Since this fibre crimp is not normal to the tows it has been modelled according to the method presented in [5]. That is, the element's coordinate systems of the finite elements placed in the crimped part of the tow are rotated to take into account for the fibre crimp.

The non-structural stitching across the length of the RUC (along X-axis) has been applied using 3D spar elements LINK180 from ANSYS® FE code.

Each colour in Figure 4 represents a different misorientation angle α. In the present study, it has been assumed that the fibre crimp varies linearly; therefore, the corresponding theoretical and the approximate rotations are calculated from the Y-coordinate of the point. The variation of the misorientation angle α relative to the maximum crimp angle β of each column of elements along the RUC length (in Y – direction) is shown in Figure 5. Notice that the rotation of the elements axis has been performed about the X-axis.

To maximize the effect of the fibre crimp due to the presence of the stitching yarns, the study has been performed assuming that all laminas are curved for the same side with maximum crimp angle of β=15º.

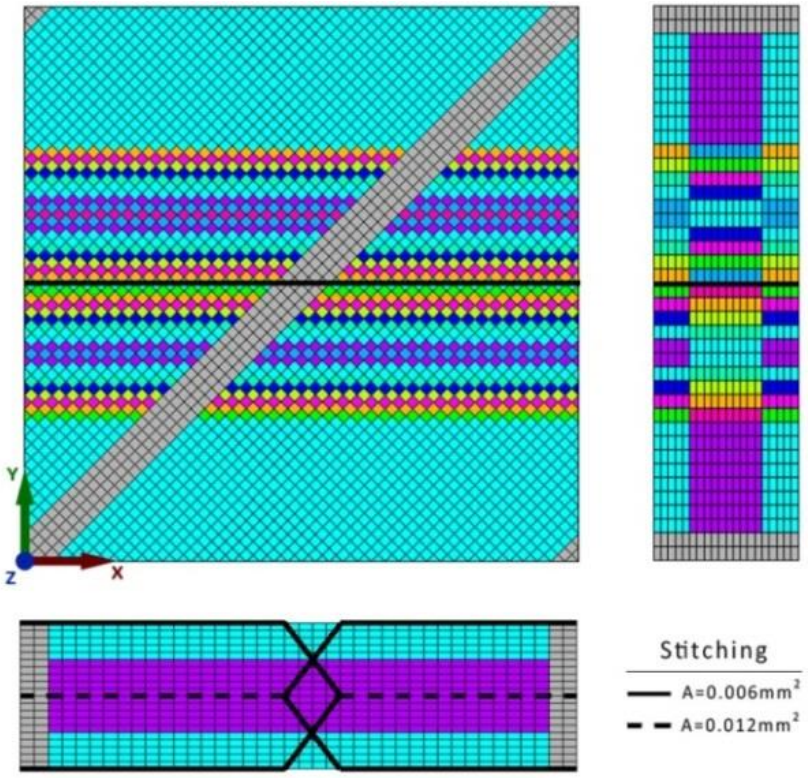

Figure 4: Stitching pattern and fibre crimp of the tows due to stitching.

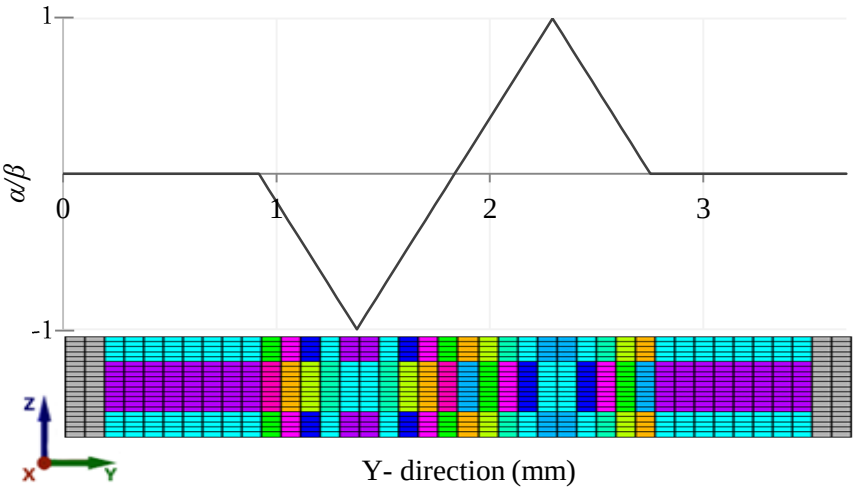

Figure 5: Variation of α/β along the Y-axis.

2.1 Mechanical properties

The mechanical properties of the tows and resin in a local coordinate system are presented in Table 3 and Table 4, respectively. The tows have been modelled as a transversely isotropic elastic material with non-linear shear behaviour. This non-linearity appears in the longitudinal and transverse through-thickness planes, 12-plane and 13-plane respectively, because in these planes, the behaviour of the tows under shear loads is controlled by the resin, whose behaviour is also non-linear [6, 7]. This non-linearity in the mechanical behaviour of the tows has been introduced in the FE model by a bilinear relationship between σ_{12}/γ_{12} and the stress-strain

curve obtained by Ditcher [8] has been taken as a reference, placing the change of slope at 60 MPa of stress and 1.4% of strain (see Table 5).

$E_{11}^t\,[GPa]$	$E_{22}^t=E_{33}^t\,[GPa]$	$\nu_{12}^t=\nu_{13}^t$	ν_{23}^t	$G_{12}^t=G_{13}^t=G_{23}^t\,[GPa]$
167.6	11.44	0.302	0.42	4.03

Table 3: Mechanical properties of the tows.

$E^m\,[GPa]$	ν^m	$G^m\,[GPa]$
3.5	0.42	1.23

Table 4: Mechanical properties of the resin.

$\sigma_{12}^*\,[MPa]$	1º Slope $\|\,G_{12}^I=G_{13}^I\,[GPa]$	2º Slope $\|\,G_{12}^{II}=G_{13}^{II}\,[GPa]$
60	4.03	0.75

Table 5: σ_{12}^* , 1º slope and 2º slope values used to define the non-linear behaviour of the tows.

$E_L^{yarn}\,[GPa]$	$E_T^{yarn}\,[GPa]$	ν^{yarn}	$G^{yarn}\,[GPa]$
61	4.2	0.29	2.9

Table 6: Mechanical properties of the stitching yarns.

The elastic constants of the stitching yarns, summarized in Table 6
Table , were obtained from FALCOM reports [9, 10] and correspond to a polyester Sinterama Zerbion® 50 dtex. Since the stitching yarns have been modelled with a uniaxial element with tension-compression capabilities, only the elastic constant E_L^{yarn} has been input in the FE code.

2.2 Boundary conditions

The boundary conditions applied to the faces of the FE model serve to simulate a tensile test in SP and ST directions (see Table 7 and Table 8). For the SP direction, a symmetry condition has been assumed in one of the faces parallel to the YZ-plane and a pure longitudinal tensile strain (along X-axis) in the opposite face. For the ST direction, a symmetry condition has been assumed in one of the faces parallel to the XZ-plane and a pure longitudinal tensile strain (along Y-axis) in the opposite face.

SP direction (warp)		
Model faces	**Boundary conditions**	**Schematic representation**
$x=0$	$u_x=0\,\|\,\sigma_{xy}=0\,\|\,\sigma_{xz}=0$	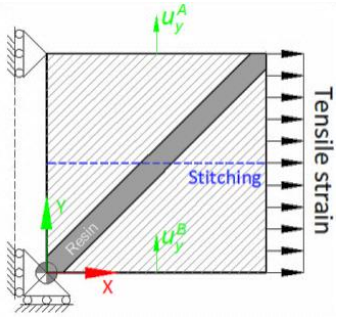
$x=a$	$\varepsilon_x=3\%\,\|\,\sigma_{xy}=0\,\|\,\sigma_{xz}=0$	

Table 7: Boundary conditions for SP (warp) direction.

ST direction (weft)		
Model faces	**Boundary conditions**	**Schematic representation**
$y=0$	$u_y=0 \mid \sigma_{xy}=0 \mid \sigma_{xz}=0$	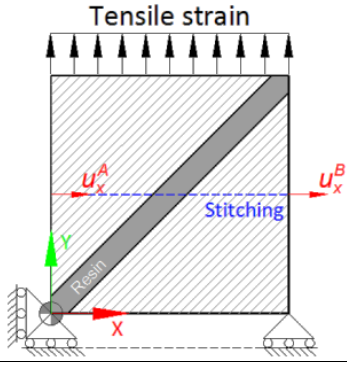
$y=a$	$\varepsilon_y=3\% \mid \sigma_{xy}=0 \mid \sigma_{xz}=0$	

Table 8: Boundary conditions for ST (weft) direction.

3 RESULTS

The numerical study showed that, if the presence of the stitching yarns and of the fibre crimp is considered, the initial tangent in-plane shear modulus G_{12}^0 for the ST direction is 6% higher than for SP direction (see Figure 6). Consequently, the shear stress-strain curves diverge from the beginning of the solution, leading to a maximum difference of 4.7% between SP and ST (see Figure 7). These results were expected since the presence of stitching yarns increases the stiffness of the FE model, especially in the ST direction.

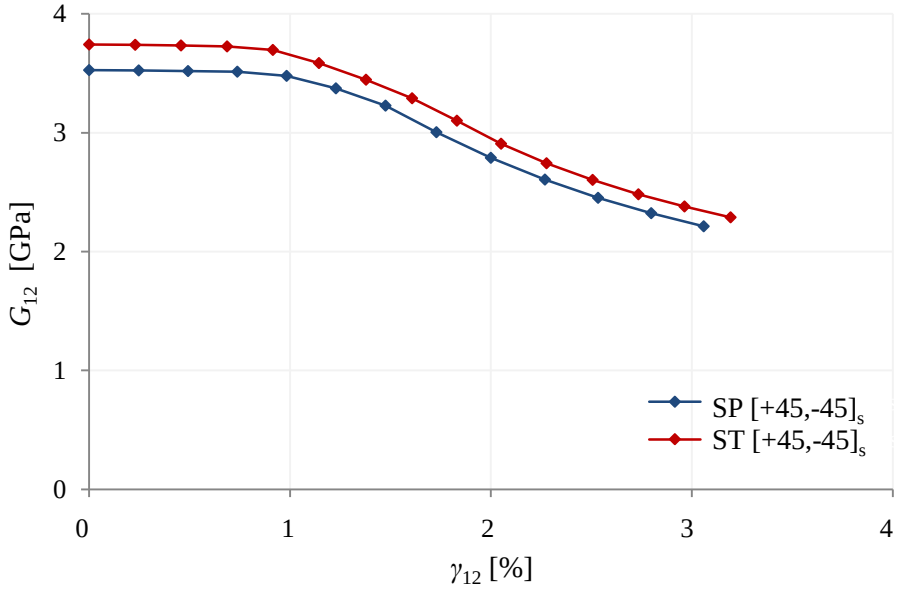

Figure 6: In-plane shear modulus G_{12} versus the in-plane shear strain γ_{12}.

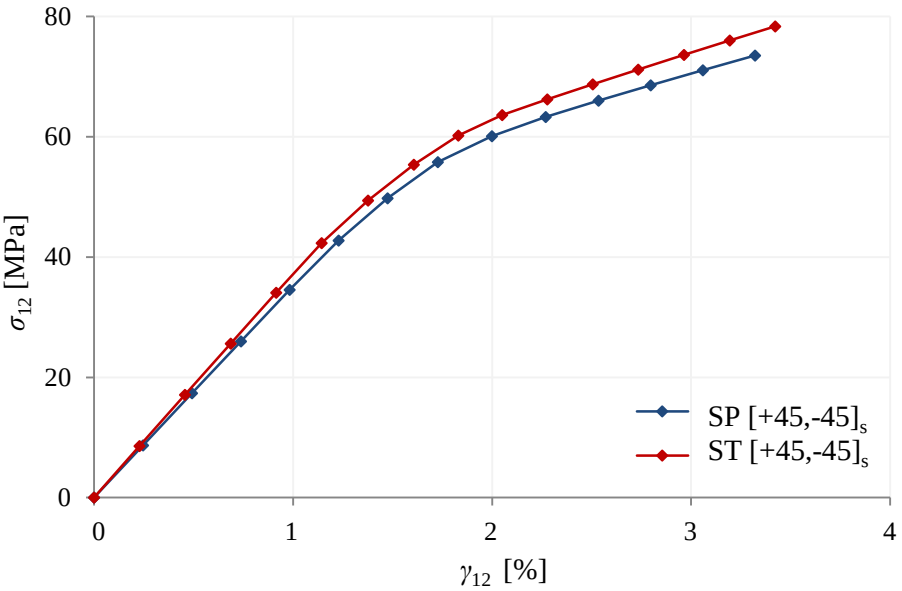

Figure 7: In-plane shear stress σ_{12} versus the in-plane shear strain γ_{12}.

Although in the numerical results, some differences can be appreciated between SP and ST directions, due to the presence of stitching yarns and to high fibre crimp angles in the thickness direction, none contributes to a difference as large as shown experimentally. Based on this evidence it was decided to review the experimental evidence in order to reassess which could be the reason(s) for such differences. A visual inspection of the panels revealed a misalignment between the nominal 0° and 90° tows in all the panels. The predominant misalignment was around 6° and almost symmetric to the stitching yarns direction (see Figures 8 and 9). Therefore, the SP and ST laminates are no longer identical from the theoretical point of view. The lowest angle between the tows was always found in the ST direction, and consequently the highest in the SP direction.

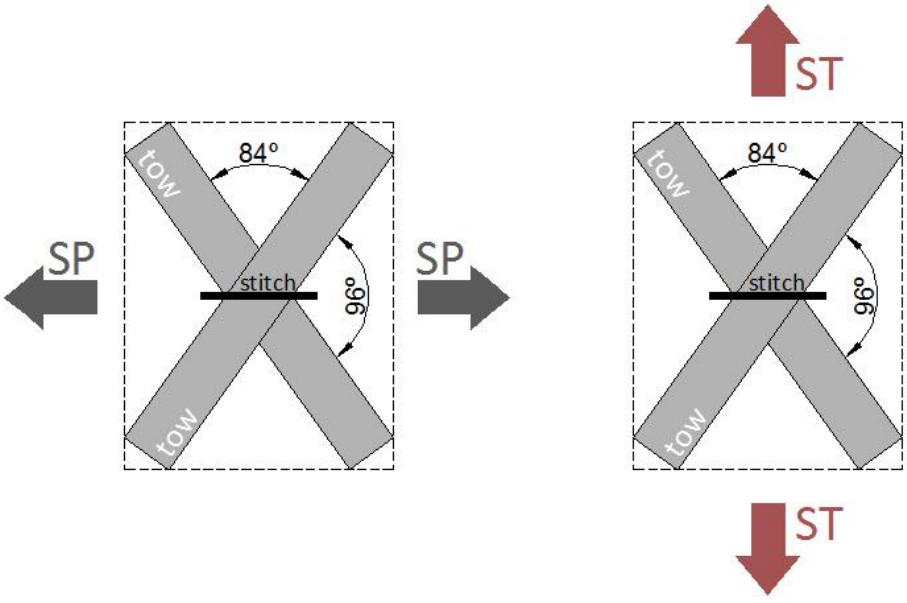

Figure 8: Schematic representation of the misalignment of 6º found in the panels between the 0º and 90º tows.

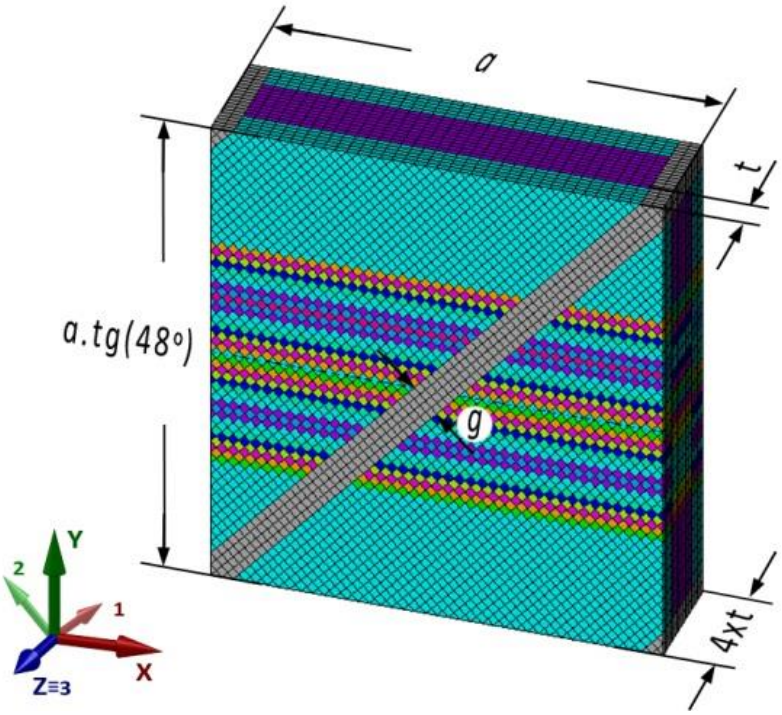

Figure 9: Dimensions employed in SP$[+48,-48]_S$ | ST$[+42,-42]_S$ NCF laminate

The numerical and the typical experimental shear stress-strain curves obtained for the SP and ST laminates are shown in Figure 10. In order to approach the numerical with the experimental results, a lamina fibre volume fraction of 67% and different values for σ_{12}^{*} and G_{12}^{II} of the non-linear behaviour of the tows had to be considered. Notice that the numerical results are represented until the moment the solution stopped to converge whereas the experimental curves are represented until the moment of failure of the laminate.

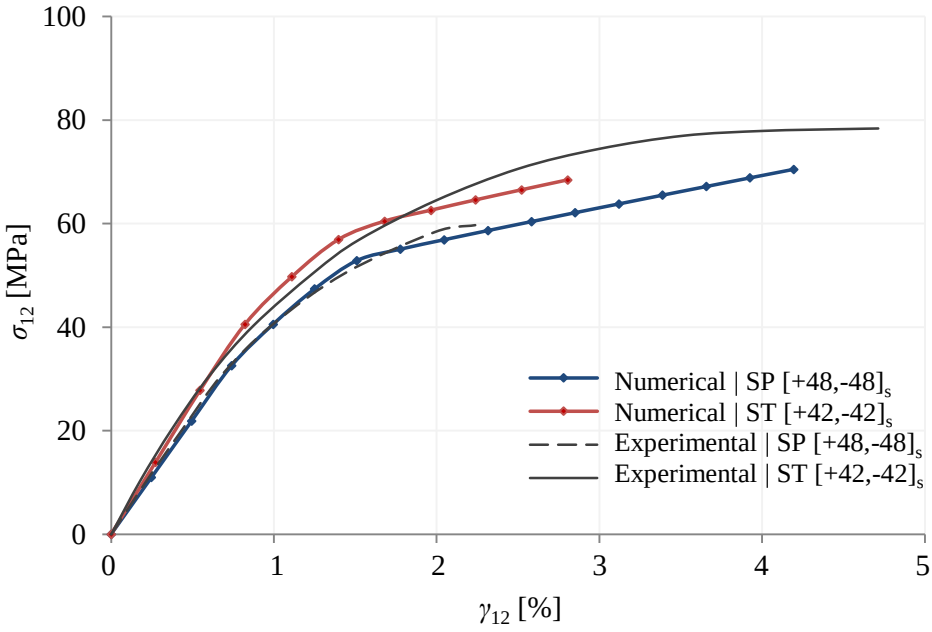

Figure 10: Numerical and typical experimental shear stress-strain curves for B-O-F-SP and B-O-F-ST laminates.

Considering a misalignment of 6º causes the shear stress-strain curves to differ a maximum of approximately 12%, which is considerably higher than what had been verified without the misalignment (around 4.7%) and presents a satisfactory agreement with the experimental results, in particular, given that the non-linear behaviour in shear that has been employed is bilinear.

4 CONCLUSIONS

The numerical analysis revealed that slightly higher shear properties are obtained in the ST direction than in SP direction if the presence of the stitching yarns and high out-of-plane crimp angles are considered. Although, the initial tangent in-plane shear modulus and the maximum shear stress-strain curves differ a maximum of approximately 6% and 4.7%, respectively, these differences are small compared with the experimental results.

A review of the experimental evidence showed that all panels presented a predominant misalignment between the nominal 0° and 90° tows of approximately 6° and almost symmetric to the stitching yarns direction and that the lowest angle between the tows was always found in the ST direction, and consequently the highest in the SP direction.

According to this evidence, FE models have been generated for both SP and ST directions with the corresponding misalignment. The results showed that the initial tangent in-plane shear modulus and the maximum shear stress-strain curves differ a maximum of approximately 14% and 12%, respectively, showing a satisfactory agreement with the experimental data obtained from the measurements made within the FALCOM project.

It has been demonstrated that the misalignment between the 0º and 90º tows is what contributes the most for the differences found in the in-plane shear performance between SP and ST laminates. Moreover, if the fibre tows are "perfectly" oriented in their nominal directions the results obtained in the both directions are very similar.

REFERENCES

[1] González A, Graciani E, Páris F. In-plane shear. FALCOM/WP3:T3.2.1/AICIA/IPS. 2005.
[2] Joffe R. Performance of non-crimp fabric composites in shear. *Key Engineering Materials*. 2010;425:45-59.
[3] Joffe R. Characterization of performance. Performance in tension. In-plane shear. FALCOM/WP3:T3.2.1/LTU/IPS. 2004.
[4] Tanaka K, Yamada M, Shinohara M, Katayama T. Effects of stitching parameters of non-crimp fabrics on the mechanical properties of CFRTP. Nagasaki2011. p. 301-4.
[5] Ferreira LM. Study of the behaviour of non-crimp fabric laminates by 3D finite element models: University of Sevilla, 2012.
[6] Drapier S, Wisnom MR. A finite-element investigation of the interlaminar shear behaviour of non-crimp-fabric-based composites. *Composites Science and Technology*. 1999;59:2351-62.
[7] Drapier S, Wisnom MR. Finite-element investigation of the compressive strength of non-crimp-fabric-based composites. *Composites Science and Technology*. 1999;**59**:1287-97.
[8] Ditcher AK. The non-linear stress-strain behaviour of carbon fibre reinforced plastic and its effects on the analysis of laminated plates and sandwich beams. Bristol, UK: University of Bristol, 1981.
[9] Puck A, Schürmann H. Failure analysis of FRP laminates by means of physically based phenomenological models. C*omposites Science and Technology*. 2002;**62**:1633-62.

[10] Baaran J. DLR structural element definition and test plan. FALCOM/WP3/DLR TECH0003. 2004.